

Experimental verification of fidelity decay: From perturbative to Fermi Golden Rule regime

R. Schäfer* and H.-J. Stöckmann

Fachbereich Physik, Philipps-Universität Marburg, Renthof 5, D-35032 Marburg, Germany

T. Gorin

Max-Planck-Institut für Physik komplexer Systeme, Nöthnitzer Str. 38, D-01187 Dresden, Germany

T. H. Seligman

*Centro de Ciencias Físicas, Universidad Nacional Autónoma de México,
Campus Morelos, C. P. 62251, Cuernavaca, Morelos, México*

(Dated: October 1, 2018)

The scattering matrix was measured for a flat microwave cavity with classically chaotic dynamics. The system can be perturbed by small changes of the geometry. We define the “scattering fidelity” in terms of parametric correlation functions of scattering matrix elements. In chaotic systems and for weak coupling the scattering fidelity approaches the fidelity of the closed system. Without free parameters the experimental results agree with random matrix theory in a wide range of perturbation strengths, reaching from the perturbative to the Fermi golden rule regime.

PACS numbers: 05.45.Mt, 03.65.Sq, 03.65.Yz

The stability of quantum motion has been a topic of increasing interest in recent years. In Ref. [1], Peres proposed to consider the time evolution of wave packets governed by two slightly different Hamiltonians. Starting from the same initial state, their overlap provides a natural measure for the stability of the quantum evolution. As “fidelity” and “quantum Loschmidt echo”, this quantity has since been investigated extensively (see Ref. [2] and references therein). Nowadays, it has become a standard benchmark for the reliability of quantum information processing [3]. Following Ref. [2], one may define fidelity as $F(t) = |f(t)|^2$ and fidelity amplitude as

$$f(t) = \langle \psi(0) | U^\dagger(t) U'(t) | \psi(0) \rangle, \quad (1)$$

where the unitary operators $U'(t)$ and $U(t)$ describe the perturbed and unperturbed time evolution of an arbitrary initial state $\psi(0)$. Depending on the strength of the perturbation one can discern three regimes. In the perturbative regime, where time-independent perturbation theory can be applied, the decay of the fidelity is Gaussian. For larger perturbations a cross-over to exponential decay is observed, with a decay constant obtained from Fermi’s golden rule [4, 5]. For very strong perturbations the decay constant saturates at the classical Lyapunov exponent [6].

Since the first spin-echo experiment by Hahn [7], echo experiments have been performed with many different quantum and classical wave systems (e.g. Ref. [8, 9]). However, wave functions are usually not accessible to experiments, and only some reduced information is available, such as the nuclear induction averaged over the probe in a magnetic resonance experiment [10, 11], or the transmission between two antennas in a microwave or ultrasound experiment [12, 13, 14].

Here, we report on the experimental measurement of fidelity decay in a flat electromagnetic cavity, using the equivalence of Helmholtz and stationary Schrödinger equation [15]. Instead of following the evolution of wave packets, we measure stationary spectra of scattering matrix elements, separately, for the perturbed and the unperturbed system. Then, for a given scattering matrix element, we compute the Fourier transform of the cross-correlation function between the two spectra. After an appropriate normalization, this defines the *scattering fidelity* amplitude. Averaging this quantity over a large number of uniformly distributed antennas with small transmission yields the standard fidelity amplitude. Yet for integrable systems, this may still lead to system specific results. For chaotic systems, by contrast, all antenna positions become equivalent and measurements for a few of them are sufficient. This statement is made more precise in [16]. Its validity is supported by our experimental results which agree with the universal prediction of random matrix theory [2, 17].

Our microwave experiments are adequately described by the statistical scattering theory [15, 18], if absorption is taken into account [19]. The scattering matrix for a billiard with two antennas can be written as:

$$S_{ab}(E) = \delta_{ab} - i V^{(a)\dagger} \frac{1}{E - H_{\text{eff}}} V^{(b)}. \quad (2)$$

Here $H_{\text{eff}} = H_{\text{int}} - (i/2) V V^\dagger$ is the effective Hamiltonian of the open system and H_{int} is the Hamiltonian of the closed billiard. The column vectors of V , denoted by $V^{(a)}$, contain the information on the coupling to the antennas at positions \vec{r}_a . For antenna diameters small compared to the wavelength, the coefficients V_{ja} are proportional to $\psi_j(\vec{r}_a)$, the wave functions of the closed system at the antenna positions.

Consider the cross-correlation function between an S-matrix element of the perturbed and the unperturbed system in the time domain:

$$\hat{C}[S_{ab}^*, S'_{ab}](t) \propto \langle \hat{S}_{ab}^*(t) \hat{S}'_{ab}(-t) \rangle, \quad (3)$$

where $S'_{ab}(E)$ is given by Eq.(2), but with H_{int} replaced by H'_{int} . The brackets denote an energy window and/or ensemble average. Note that $\hat{C}[S_{ab}^*, S'_{ab}](t)$ describes a kind of echo-dynamics, which is similar to the quantum echo defined in Eq. (1), but decays even without any perturbation. We therefore use the autocorrelation function for a heuristic normalization and define the scattering fidelity amplitude as

$$f_{ab}(t) = \frac{\hat{C}[S_{ab}^*, S'_{ab}](t)}{\sqrt{\hat{C}[S_{ab}^*, S_{ab}](t) \hat{C}[S'_{ab}^*, S'_{ab}](t)}}. \quad (4)$$

Reflection and transmission measurements have been performed in a flat microwave cavity, with top and bottom plate parallel to each other [20]. The cavity is quasi-two-dimensional for frequencies $\nu < c/(2h)$, where h is the height of the billiard. The billiard is shown in the insert of Fig. 1. It consists of a rectangular cavity of length $L = 438$ mm, width $B = 200$ mm and height $h = 8$ mm, a quarter-circle insert of radius $R_1 = 70$ mm, and a half-circle insert of radius $R_2 = 60$ mm placed on the lower side. The position of the latter was changed in steps of 20 mm to generate an ensemble average over 15 different systems. Additional elements were inserted into the billiard to suppress bouncing-ball resonances: two half-circle inserts with radius $R_3 = 30$ mm, and a slope on the upper boundary. The perturbation of the system was achieved by varying the length L in steps of $l = n \cdot 0.2$ mm, with $n = 1-10$. The change of area and surface due to the shift of the billiard wall, was taken into account by unfolding the spectra to a mean level distance of one. The frequency window of the Fourier transforms was 1 GHz wide, and a Welch filter was applied. In this range the antenna coupling and the wall absorption are approximately constant.

We compare the experimental results with the random matrix prediction

$$f(t) = \exp\left[-4\pi^2\lambda^2\left(t^2 + \frac{t}{2} - \int_0^t \int_0^\tau b_2(\tau') d\tau' d\tau\right)\right]. \quad (5)$$

This expression is obtained by exponentiation of the linear response result, thus incorporating the known behavior in both, the perturbative and the Fermi golden rule regime [17]. Here, λ is the perturbation strength, and $b_2(t)$ is the two-point form factor for the Gaussian orthogonal ensemble. We use dimensionless units, where the Heisenberg time $t_H = \hbar/\Delta$ is equal to one and Δ denotes the mean level spacing.

Figure 1 shows on a logarithmic scale the cross-correlation function $\hat{C}[S_{11}^*, S'_{11}](t)$ given in Eq. (3) together with the autocorrelation function $\hat{C}[S_{11}^*, S_{11}](t)$.

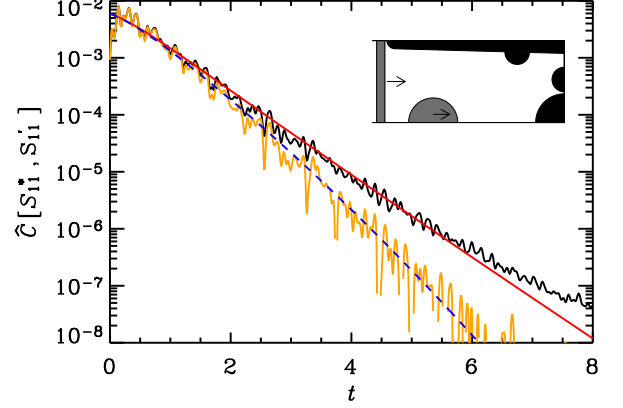


FIG. 1: (Color online): Logarithmic plot of the correlation function $\hat{C}[S_{11}^*, S'_{11}]$ for $\nu = 5-6$ GHz, $l = 1$ mm and $\lambda = 0.047$. The experimental results for the auto correlation are shown in black, while the correlation of perturbed and unperturbed system are shown in gray / orange. The smooth solid curve corresponds to the theoretical auto-correlation function, and the dashed curve to the product of auto-correlation function and fidelity amplitude. The insert shows the billiard geometry used. Moveable parts are marked with an arrow. See text for dimensions.

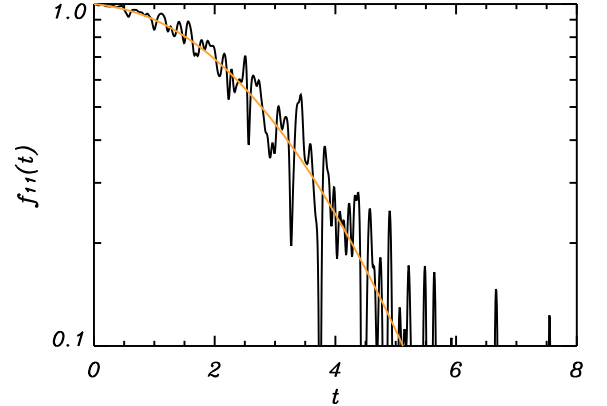


FIG. 2: (Color online): Logarithmic plot of the scattering fidelity amplitude $f_{11}(t)$ for $\nu = 5-6$ GHz, $l = 1$ mm and $\lambda = 0.047$. The smooth curve shows the linear-response result for the fidelity amplitude $f(t)$, where the perturbation strength λ was obtained from the variance of the level velocities.

The latter agrees with the corresponding theoretical autocorrelation function, calculated in [19]. The parameters for the wall absorption and the coupling of the antennas have been obtained according to the same reference. With increasing time, $\hat{C}[S_{11}^*, S'_{11}](t)$ deviates more and more from the autocorrelation function. This deviation contains the essential information on echo dynamics.

For the frequency range shown in Fig. 1, the pertur-

bation strength λ was determined directly from the measured spectra via the variance of the level velocities. The dashed curve in Fig. 1 is a product of the theoretical autocorrelation function and the fidelity amplitude (Eq. (5)) of the closed system. The experimental result for the cross-correlation function (Eq. (3)) agrees perfectly over six orders of magnitude with the linear-response expression without any free parameter. This justifies our definition of the scattering fidelity amplitude $f_{ab}(t)$ in Eq. (4).

Figure 2 shows $f_{ab}(t)$, computed from the experimental cross- and autocorrelation functions according to Eq. (4). There are two advantages for using the experimental and not the theoretical autocorrelation function: The computed quantity does not depend on theoretical assumptions, and the influence of non-generic features, visible in the correlation functions, is reduced.

We now study the dependence of the fidelity decay on the perturbation strength. In our experiment λ varies from $\lambda = 0.01$ for $n = 1$ and $\nu = 3-4$ GHz up to $\lambda = 0.5$ for $n = 10$ and $\nu = 17-18$ GHz. Figure 3 shows the scattering fidelity amplitude for three different frequency windows. Here, λ has been fitted to the experimental curves, as its determination from the level dynamics is time consuming and for strong perturbations not always feasible. To improve statistics, experimental results for f_{11} , f_{22} and f_{12} have been superimposed.

For the random matrix model one expects a transition from linear to quadratic decay near the Heisenberg time. In the perturbative regime, the linear term in the exponential is still close to one and we observe Gaussian decay of the fidelity amplitude, as seen in Fig. 3(a). With increasing perturbation strength the linear term becomes more pronounced, leading to the Fermi golden rule regime [4, 5]. The (exponentiated) linear-response formula (5) agrees very well with experiment throughout the range. Recently, an exact solution for the random matrix model proposed in [17] has been obtained using supersymmetry techniques [21]. This result is shown as dashed lines in Fig. 3. For the accessible perturbation strengths the experiment does not allow to distinguish between the linear-response and the exact result.

In billiard systems, the parameter variation is not due to a change of the Hamiltonian, but of the boundary condition. It was shown in chapter 5 of Ref. [15] that both situations are equivalent. For the case of a parameter variation in the billiard due to a shift of a straight wall the matrix element of the equivalent perturbation reads

$$(H_1)_{nm} = l \int_0^B \frac{\partial \psi_n(x, y)}{\partial x} \frac{\partial \psi_m(x, y)}{\partial x} \Big|_{x=0} dy, \quad (6)$$

where l is the shift of the wall (in x -direction) and B is the length of the shifted wall. The perturbation strength according to the random matrix model in [17] is given by the variance of the off-diagonal matrix elements:

$$\lambda^2 = \left\langle [(H_1)_{nm}]^2 \right\rangle. \quad (7)$$

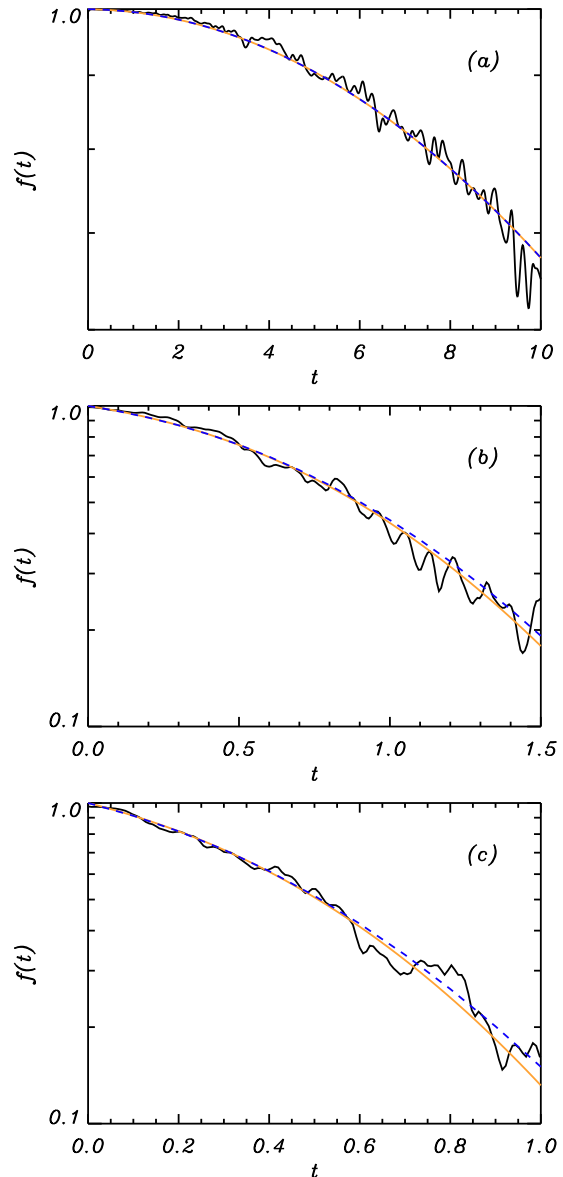


FIG. 3: Logarithmic plot of the fidelity amplitude $f(t)$ for three different perturbation strengths. Linear response result (smooth solid gray line), exact theoretical result (dark dashed line), and experimental result (solid dark line). The perturbation parameter λ has been fitted to each experimental curve. The parameters were $\nu = 3-4$ GHz, $l = 0.4$ mm, $\lambda = 0.01$ for (a), $\nu = 13-14$ GHz, $l = 0.6$ mm, $\lambda = 0.13$ for (b), and $\nu = 16-17$ GHz, $l = 0.8$ mm, $\lambda = 0.21$ for (c).

Using Berry's conjecture of the superposition of plane waves [22] we can derive for large wave numbers k :

$$\lambda^2 = \frac{2L}{3\pi^3} k^3 l^2 = \frac{16L}{3c^3} \nu^3 l^2. \quad (8)$$

In Ref. [23], the same expression has been obtained using periodic orbit theory and the ergodicity assumption.

Figure 4 shows the experimental perturbation strength

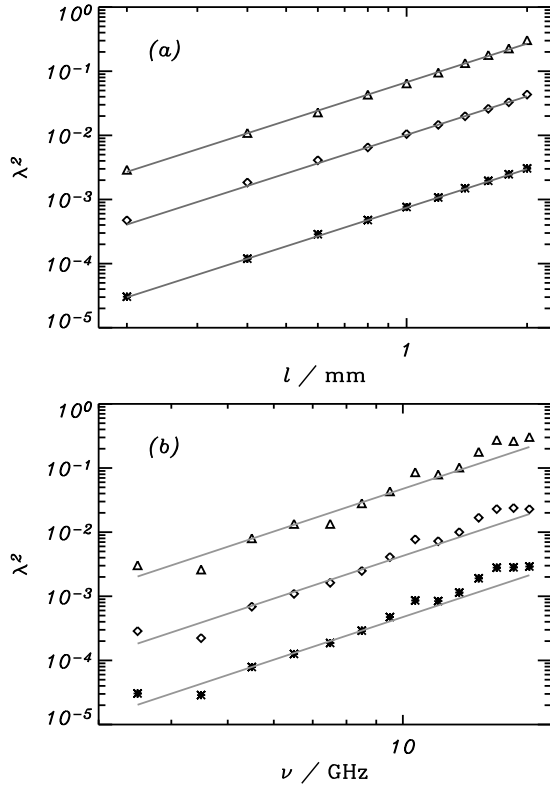


FIG. 4: (a) Perturbation strength λ^2 as a function of the shift l of the billiard wall for the frequency windows $\nu = 3$ –4 (stars), 9–10 (diamonds) and 16–17 GHz (triangles). The slope of the straight lines is 2. (b) λ^2 as a function of the frequency ν for $l = 0.2$ (stars), 0.6 (diamonds) and 2.0 mm (triangles). The slope of the straight lines is 3.

λ^2 as a function of the shift l of the billiard wall for three different frequency regimes (a), and as a function of the frequency, for three different shifts (b). We observe excellent agreement with the scaling $\lambda^2 \propto l^2 \nu^3$ predicted in Eq. (8). This can be used to average all experimental data as a function of the scaled variable $4\pi^2 \lambda^2 C(t)$, thus reducing the fluctuations almost completely [16]. In spite of the correct scaling, the experimental prefactor is about three times smaller than predicted. In cases where we determined the variance of level velocities directly from the measured spectra, we found the same discrepancy. The deviation is caused by the fact that we are far from the semiclassical limit, for which Eq. (8) was derived. Additional numerical studies for the Sinai billiard by H. Schanz [24] substantiate this explanation.

We have shown that the fidelity amplitude $f_{ab}(t)$ of scattering matrix elements S_{ab} is an easily accessible quantity. In our experiment it approximates the ordinary fidelity amplitude $f(t)$. The relevant parameters are well controlled. This enabled us to verify the theoretical results for fidelity decay covering the range from

the perturbative to the Fermi golden rule regime without any free parameter. For strong perturbations the exact solutions of random matrix theory predict a revival of the fidelity amplitude at the Heisenberg time, whereas semiclassics predicts an exponential decay with the Lyapunov exponent up to the Ehrenfest time [6]. It remains an open question, whether these features can be verified in a future microwave experiment.

T Prosen, U Kuhl and H Schanz are thanked for helpful discussions taking place in part on occasion of a workshop at the Centro Internacional de Ciencias in Cuernavaca, Mexico. T.H.S. acknowledges support under the grants DGAPA 10803 and CONACyT 41000-F. The experiments were supported by the Deutsche Forschungsgemeinschaft.

* rudi.schaefer@physik.uni-marburg.de

- [1] A. Peres, Phys. Rev. A **30**, 1610 (1984).
- [2] T. Prosen, T. H. Seligman, and M. Žnidarič, Prog. Theor. Phys. Suppl. **150**, 200 (2003).
- [3] M. A. Nielsen and I. L. Chuang, *Quantum Computation and Quantum Information* (University Press, Cambridge, 2000).
- [4] P. Jacquod, P. G. Silvestrov, and C. W. J. Beenakker, Phys. Rev. E **64**, 055203 (2001).
- [5] N. R. Cerruti and S. Tomsovic, Phys. Rev. Lett. **88**, 054103 (2002).
- [6] R. A. Jalabert and H. M. Pastawski, Phys. Rev. Lett. **86**, 2490 (2001).
- [7] E. L. Hahn, Phys. Rev. **80**, 580 (1950).
- [8] N. A. Kurnit, I. D. Abella, and S. R. Hartmann, Phys. Rev. Lett. **13**, 567 (1964).
- [9] F. B. J. Buchkremer *et al.*, Phys. Rev. Lett. **85**, 3121 (2000).
- [10] S. Zhang, B. H. Meier, and R. R. Ernst, Phys. Rev. Lett. **69**, 2149 (1992).
- [11] H. M. Pastawski, P. R. Levstein, and G. Usaj, Phys. Rev. Lett. **75**, 4310 (1995).
- [12] G. Lerozey *et al.*, Phys. Rev. Lett. **92**, 193904 (2004).
- [13] A. Derode, P. Roux, and M. Fink, Phys. Rev. Lett. **75**, 4206 (1995).
- [14] O. I. Lobkis and R. L. Weaver, Phys. Rev. Lett. **90**, 254302 (2003).
- [15] H.-J. Stöckmann, *Quantum Chaos - An Introduction* (University Press, Cambridge, 1999).
- [16] R. Schäfer, T. Gorin, T. H. Seligman, and H.-J. Stöckmann, New J. Phys. **7**, 152 (2005).
- [17] T. Gorin, T. Prosen, and T. H. Seligman, New J. Phys. **6**, 20 (2004).
- [18] C. Mahaux and H. A. Weidenmüller, *Shell-Model Approach to Nuclear Reactions* (North-Holland, Amsterdam, 1969).
- [19] R. Schäfer, T. Gorin, T. H. Seligman, and H.-J. Stöckmann, J. Phys. A **36**, 3289 (2003).
- [20] U. Kuhl, E. Persson, M. Barth, and H.-J. Stöckmann, Eur. Phys. J. B **17**, 253 (2000).
- [21] H.-J. Stöckmann and R. Schäfer, New J. Phys. **6**, 199 (2004).

- [22] M. V. Berry, J. Phys. A **10**, 2083 (1977).
- [23] P. Lebœuf and M. Sieber, Phys. Rev. E **60**, 3969 (1999).
- [24] H. Schanz, Private communication, 2004.